



Modelling of Mechanical and Mechatronic Systems MMaMS 2014

Contact Problems Between the Hub and the Shaft with a Three-Angular Shape of Cross-Section for Different Angular Positions

Marian Dudziak^{a,c}, Grzegorz Domek^b, Andrzej Kołodziej^{a*}, Krzysztof Talaśka^c

^a Technical Institute, Higher Vocational State School in Kalisz, Kalisz, 62-800, Poland

^b Faculty of Mathematics, Physics & Technical Sciences, Kazimierz Wielki University in Bydgoszcz, Bydgoszcz, 85-092 Poland

^c Chair of Basics of Machine Design, Poznan University of Technology, Poznan, 60-965, Poland

Abstract

The actual state of the macrogeometry of the surfaces of mating elements, particularly form deviations, has a direct influence on constructional features and the functionality of the connections which are applied in mechanical engineering. The authors made an attempt to assess the influence of radial deviations, cross-section deviations and their compilations on the occurrence of the variable values of local stresses and displacements which are caused by the limited contact zone in the connection. The contact problems are represented on the example of the numerical simulation of the contact between rigid and non-deformable hub and the shaft with a three-angular cross-section and a saddleback distortion for different angular positions of the shaft. The authors have proved the occurrence of variable relative stresses and contact pressures. The authors have also showed the convergence of the calculated values of the forces and moments which are needed to move and rotate the shaft in the hub with the values obtained during the experimental investigations which were performed in advance.

© 2014 The Authors. Published by Elsevier Ltd. This is an open access article under the CC BY-NC-ND license (<http://creativecommons.org/licenses/by-nc-nd/3.0/>).

Peer-review under responsibility of organizing committee of the Modelling of Mechanical and Mechatronic Systems MMaMS 2014

Keywords: form deviations; static analysis with the FEM; axisymmetrical connections;

1. Introduction

This elaboration is an effect of the analysis of the state of the recording and the execution of the axisymmetrical constructions which are manufactured for the needs of the present productions of the automotive industry,

* Corresponding author. Tel.: +48 62-767-9685; fax: +48 62-767-9581.

E-mail address: a.kolodziej@ip.pwsz.kalisz.pl

aircraft industry and partly engineering industry. The irregularities of the surfaces with special taking into account the form deviations were investigated. These irregularities are responsible for the existing size of the contact area of mating elements, i.e. the shaft and hub. For many cases the size of the contact area is the reason of the decreasing the assumed strength criteria, tribological criteria and safety criteria. Form deviations determine the area and distribution of contact points, clearance between individual spots of mating surfaces and local contact pressures which can be a source of vibrations [1, 2].

The measurements which were carried out during the production of connection elements and other axisymmetrical constructions, have showed the occurrence of manufacturing deviations of the shaft and hub in transverse and longitudinal sections. These deviations have formed different geometric configurations for variable deviations of the roundness and cylindricity. Figure 1 presents different contact areas for the connection of the shaft and hub.

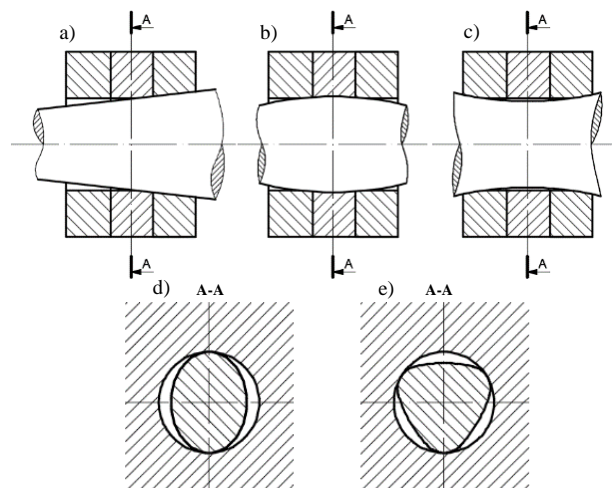


Fig. 1. The scheme of the connection of the shaft and hub: a) conicity, b) crowning, c) saddle back distortion; d) ovality, e) three-angular cross-section

From the operation point of view, the continuity of the contact zone is required, but form errors of individual elements of the connection allow only for the cooperation on the limited area of the mating elements. The presented examples of the form errors of the shaft and hub considerably restrict the assumed strength features and functional-operating features of the designed and manufactured connections.

2. Experimental investigations

For the needs of the experimental investigations, the cylindrical elements with variable geometry in longitudinal and transverse sections were manufactured. The following rollers were made with: nominal (rectangle) longitudinal section - nominal circle in transverse section, nominal (rectangle) - oval, nominal (rectangle) - three-angular, saddleback - nominally round, saddleback - oval, saddleback - three-angular, crowning - nominally round, crowning - oval, crowning - three-angular, conical - nominally round, conical - oval, conical - three-angular.

Two series of shafts with the diameter $\phi 19$ mm and length $L = 70$ mm were manufactured with model deviations of the shape (material 40HM, hardness 40 HRC) – fig. 2. The first series of shafts had the tolerated diameter $\phi 19h6$ (the value of the tolerance $T_w = 13 \mu\text{m}$) and the second series had the tolerated diameter $\phi 19h9$ (the value of the tolerance $T_w = 52 \mu\text{m}$). The shafts with the variable geometry were measured with the application of the special-purpose instrument for the measurement of form deviations, i.e. Hommel - Etamic Roundscan 535.

Next, the investigations of the actual capacity of the transmission of the given operation load were performed. In order to do this, the experimental test stand for the measurement of the axial force of friction and the moment of

friction between the hub and shaft with the application of extensometer was designed and built. A basic element of the test stand is the pilot sleeve with the diameter $\varnothing 19$ mm which was manufactured with the deviation of cylindricity below $1 \mu\text{m}$ (material 40HM, hardness 50 HRC). The sleeve was mated with the measured model shafts with variable geometry.

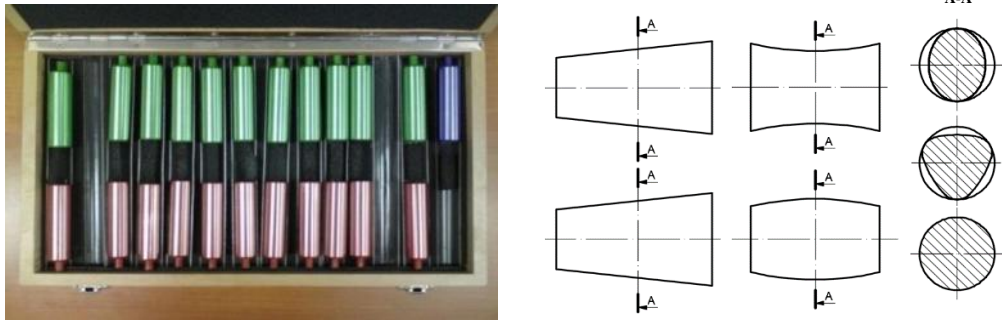


Fig. 2. The composition of model shafts: a) first series, $T_w = 0.013$ mm (green colour), b) second series, $T_w = 0.052$ mm (pink colour), c) nominal shaft $T_w = 0.001$ mm (blue colour)

The measurements of the axial force of friction and the moment of friction of the shafts with a saddleback distortion in longitudinal section and a three-angular cross-section were performed for five angular positions in the sleeve: 0° , 45° , 90° , 135° and 180° . The results of the experimental measurements of variations of frictional resistance during the rotation and the displacements of the shafts with different versions of the shape and the angular positions in the sleeve were confirmed by means of the numerical simulations which allowed to determine the reduced Huber -Mises stresses.

The contact problems are shown on the example of the numerical simulation of the contact between the saddleback shaft with three-angular cross-section and the rigid and non-deformable sleeve (fig. 1. c, e).

3. Numerical research

During the numerical modelling of the shaft-hub connection, some assumptions were made to simplify the numerical model, e.g. the symmetry of the model. The simplification consists in the acceptance of the half of the weight of the shaft (fig. 3b), and the contact between the mating surfaces of the shaft and hub is analysed only on the length 1 mm from one end of the connection. The shaft has a three-angular cross-section with the tolerance $T_w = 13 \mu\text{m}$ (fig. 3c).

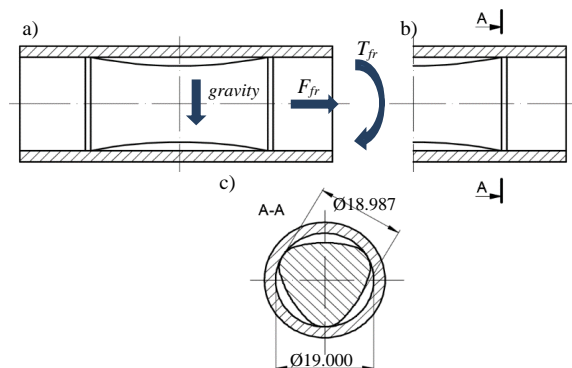


Fig. 3. The stages of the simplification of the physical model: a) full model, b) reduced model with the symmetry, c) reduced model with the limited contact length between the shaft and hub, T_{fr} - the moment of friction, F_{fr} - the force of friction

For the purpose of the determination of the required force to disassembly the connection, it is necessary to obtain the values of the reactions in contact points between the shaft and hub and the values of the coefficient of friction. The value of the coefficient of friction was obtained experimentally and was equal $\mu = 0.12$. On the basis of the value of the force of friction and geometric features of the connection, we can determine the value of the moment of friction to disassembly the connection.

3.1. The numerical model

Figure 4 presents the numerical model with generated mesh (2D elements: CPS4R). The shaft was placed in the hub which was modelled as a rigid plane [3-5]. The mesh was refined in the area of tops of the three-angular profile of the cross-section (fig. 4). The contact was defined between the surfaces of the shaft and hub - the value of the coefficient of friction was equal $\mu = 0.12$. The load was defined as a half of the weight of the shaft. The plane of the hub was fixed.

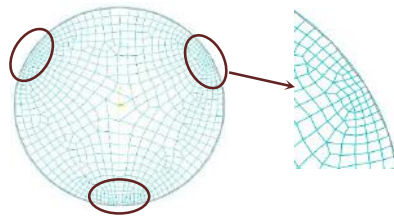


Fig. 4. Numerical model - digitized, the shaft-hub connection

The analyses were carried out for five angular positions of the shaft in the hub. The first position, defined as 0° corresponds to the support of the shaft on one top. Such angular position of the shaft is presented in Figures 3c and 4. The properties of material are the following: Young's modulus $E = 210 \text{ GPa}$, Poisson coefficient $\nu = 0.3$, density of steel 7830 kg/m^3 .

3.2. The results of the numerical investigations

As a result of the numerical investigations we received the state of the reduced stresses (Mises stresses), the values of contact pressures in contact points, the values of the reactions and the values of forces of friction and moments of friction which are necessary to disassembly the position of connection elements.

The position 0°

Figure 5 presents the state of the reduced stresses (Mises stresses) with the indication of the place of the occurrence of maximum stresses for the angular position 0° of the shaft. The values of the reactions and their components at the shaft supports are also presented. Figure 6 presents the values and spots of the concentration of contact pressures.

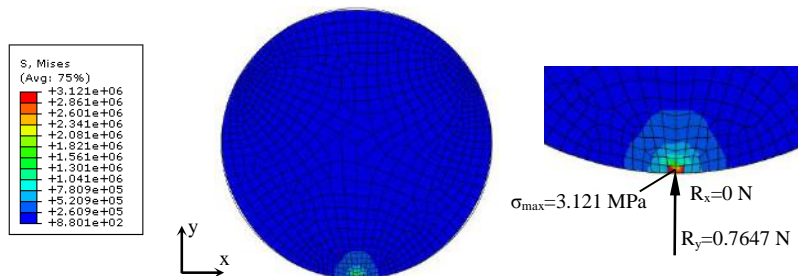


Fig. 5. Spots of the concentration of the reduced stresses (Mises stresses) and reaction components at the supports of the shaft for the angular position 0°

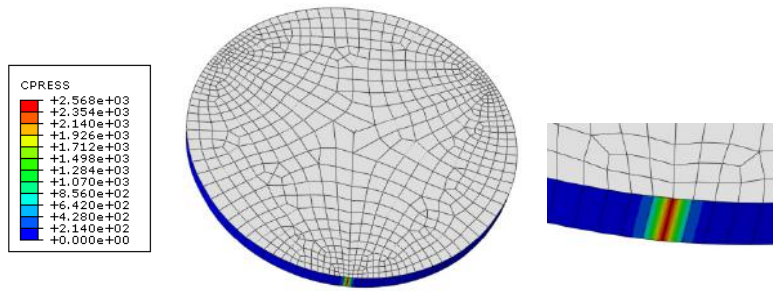


Fig. 6. The values and spots of the concentration of contact pressures for the angular position 0°

The position 45°

Figure 7 presents the state of the reduced stresses (Mises stresses) with the indication of the place of the occurrence of maximum stresses for the angular position 45° of the shaft. The values of the reactions and their components at the shaft supports are also presented. Figure 8 presents the values and spots of the concentration of contact pressures.

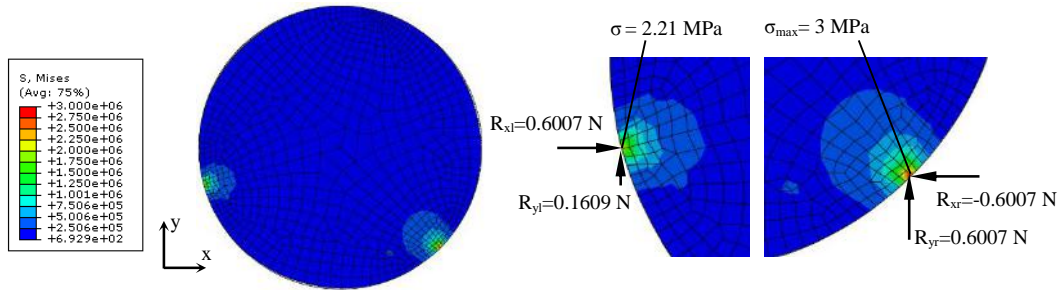


Fig. 7. Spots of the concentration of the reduced stresses (Mises stresses) and reaction components at the supports of the shaft for the angular position 45°

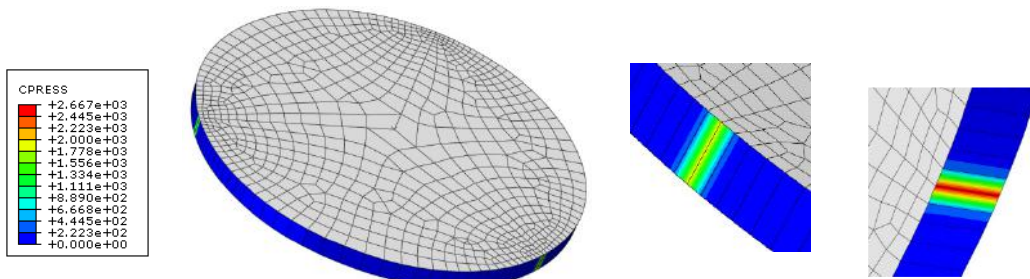


Fig. 8. The values and spots of the concentration of contact pressures for the angular position 45°

The position 90°

Figure 9 presents the state of the reduced stresses (Mises stresses) with the indication of the place of the occurrence of maximum stresses for the angular position 90° of the shaft. The values of the reactions and their components at the shaft supports are also presented. Figure 10 presents the values and spots of the concentration of contact pressures.

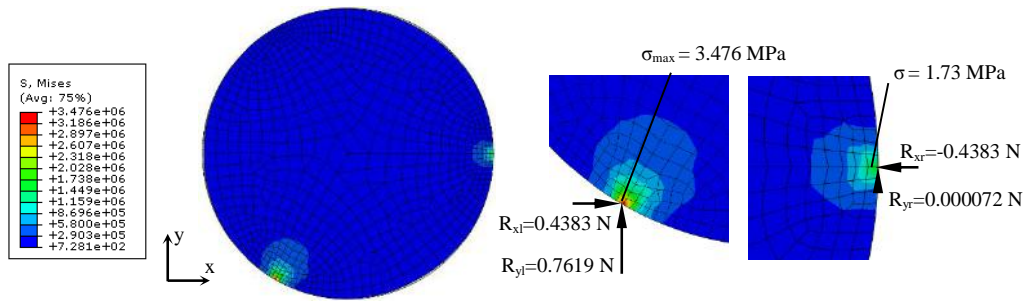


Fig. 9. Spots of the concentration of the reduced stresses (Mises stresses) and reaction components at the supports of the shaft for the angular position 90°

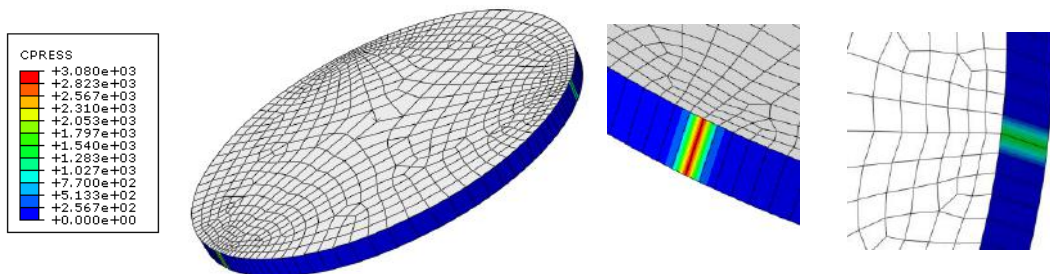


Fig. 10. The values and spots of the concentration of contact pressures for the angular position 90°

The position 135°

Figure 11 presents the state of the reduced stresses (Mises stresses) with the indication of the place of the occurrence of maximum stresses for the angular position 135° of the shaft. The values of the reactions and their components at the shaft supports are also presented. Figure 12 presents the values and spots of the concentration of contact pressures.

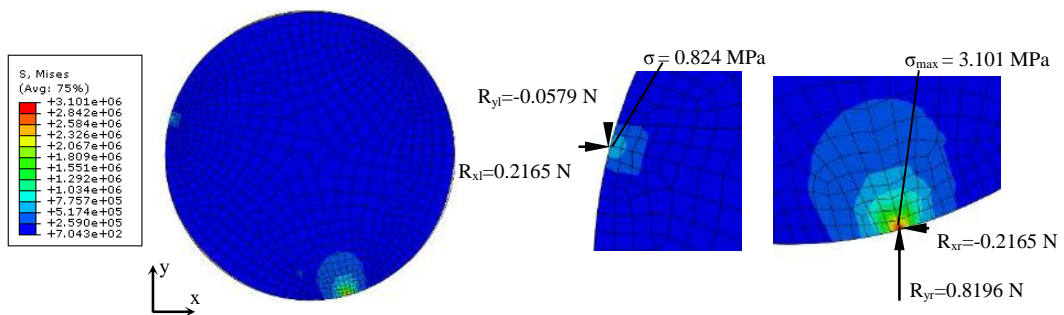


Fig. 11. Spots of the concentration of the reduced stresses (Mises stresses) and reaction components at the supports of the shaft for the angular position 135°

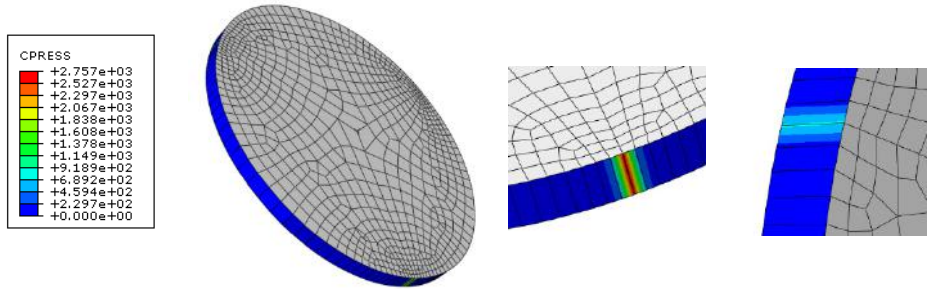


Fig. 12. The values and spots of the concentration of contact pressures for the angular position 135°

The position 180°

Figure 13 presents the state of the reduced stresses (Mises stresses) with the indication of the place of the occurrence of maximum stresses for the angular position 180° of the shaft. The values of the reactions and their components at the shaft supports are also presented. Figure 14 presents the values and spots of the concentration of contact pressures.

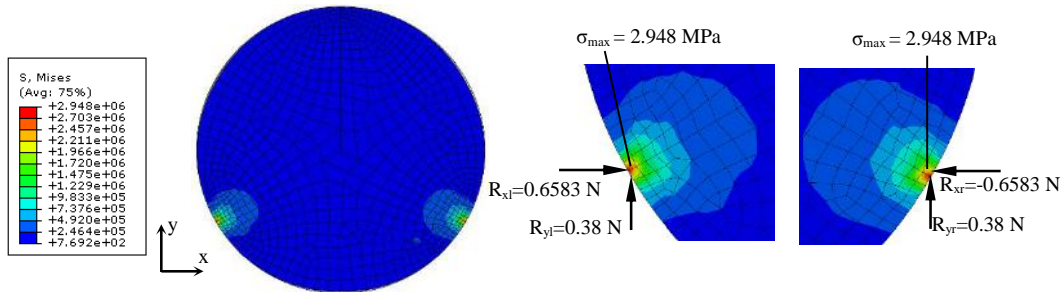


Fig. 13. Spots of the concentration of the reduced stresses (Mises stresses) and reaction components at the supports of the shaft for the angular position 180°

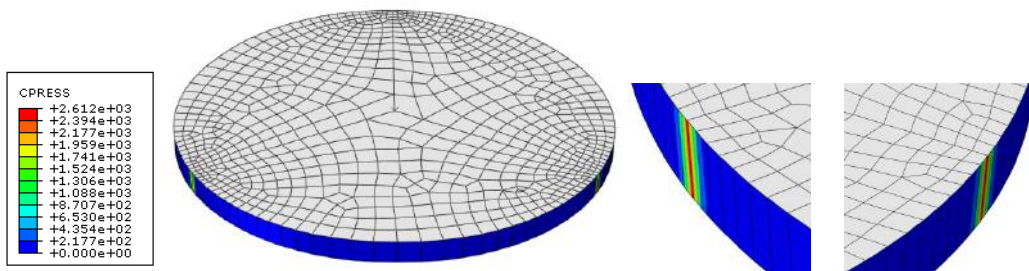


Fig. 14. The values and spots of the concentration of contact pressures for the angular position 180°

Table 1 presents the list of component reactions, resultant reactions, forces of friction and moments of friction. Figure 15 shows the graphic representation of the reduced stresses (Mises stresses) and contact pressures in the function of the angular position of the shaft.

Table 1. The list of the results of reactions and forces of friction and moments of friction for different angular positions of the shaft with a three-angular cross-section

	The position of the shaft axis				
	0°	45°	90°	135°	180°
Horizontal reaction R_{xl}	0	0.6007	0.4383	0.2165	0.6583
Horizontal reaction R_{xr}	0	-0.6007	-0.4383	-0.2165	-0.6583
$(R_{xl} + R_{xr})$	0.0	0.0	0.0	0.0	0.0
Vertical reaction R_{yl}	-----	0.1609	0.7619	-0.0579	0.3800
Vertical reaction R_{yr}	-----	0.6007	0.000072	0.8196	0.3800
$(R_{yl} + R_{yr})$	0.7647	0.7617	0.761972	0.7617	0.7600
Resultant reaction R_l	-----	0.621876	0.878976	0.224109	0.760105
Resultant reaction R_r	-----	0.849589	0.4383	0.847712	0.760105
$R_l + R_r$	0.7647	1.471464	1.317276	1.071821	1.520209
Force of friction F_{fr} [N] (for shaft displacement)	0.183528	0.353151	0.316146	0.257237	0.36485
Moment of friction T_{fr} [Nm] (for shaft rotation)	0.001744	0.003355	0.003003	0.002444	0.003466

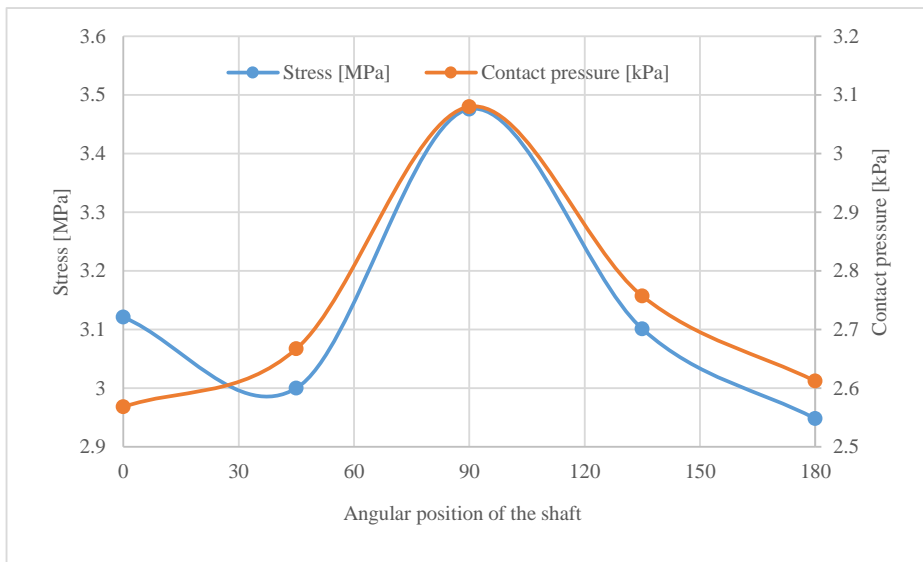


Fig. 15. Reduced stresses (Mises stresses) and contact pressures in the function of the angular position of the shaft

4. Conclusions

1. The results of the numerical simulations have confirmed the variation of the values of the reduced stresses (Mises stresses) and contact pressures in the function of the angular position of the shaft.
2. The results of the numerical simulations have confirmed the variation of the force of friction and the moment of friction in the function of the angular position of the shaft.
3. The highest values of the force of friction and the moment of friction are for the angular position 180° of the shaft - this corresponds to the uniform load of two tops of the cross-section.

4. The non-uniform values of the force and moment of friction are the sources of vibrations in the moving axisymmetrical connections.

References

- [1] S. Adamczak, Geometrical measurements of surface – shape, waviness and roughness, WNT, Warsaw, 2008.
- [2] S. Adamczak, W. Makiela, K. Stępień, Investigating advantages and disadvantages of the analysis of a geometrical surface structure with the use of Fourier and wavelet transform, *Metrology and Measurement Systems XVII* (2) (2010) 233-244.
- [3] D. Croccolo, M. de Agostinis, N. Vincenzi, Design and optimization of shaft-hub hybrid joints for lightweight structures: Analytical definition of normalizing parameters, *International Journal of Mechanical Sciences* 56 (1) (2012) 77-85.
- [4] P.B. Dhanish, J. Mathew, A fast and simple algorithm for evaluation of minimum zone straightness error from coordinate data, *International Journal of Advances Manufacturing Technology* 32 (2007) 92-98.
- [5] S. Sen, B. Aksakal, Stress analysis of interference fitted shaft-hub system under transient heat transfer conditions, *Materials & Design* 25 (5) (2004) 407-417.